A Details in A^2

A.1 Unify Magnitude of Perturbations

Perturbations generated by different operations in O_p have different magnitudes and thus require different magnitudes of step size for different o_p. For example, *FGSM* generates perturbations with elements belonging to $\{-1, 0, 1\}$, while the perturbation generated by *FGM* is usually in the magnitude of 10^{-3}. Obviously, they cannot use the same step size. To have a uniform effect of the step size block, we normalize the magnitude of other generated perturbations to be the same as *FGSM* (i.e., $\delta_{o_p} = \delta_{o_p} \cdot \frac{\|\delta_{FGSM}\|}{\|\delta_{o_p}\|}$). In this way, we find that other attack methods such as *FGM* can achieve good results with the same step size as *FGSM*.

A.2 Temperature Parameter in *Softmax*

Since there is an order of magnitude difference in step size operations, the larger step size with the same score will dominate the output. For example, $0.7 \cdot 10^{-2}\eta + 0.3 \cdot \eta \approx 0.3\eta$. The output of the step size block is dominated by the operation η, despite the greater weight of $10^{-2} \cdot \eta$. To alleviate the problem, we use the temperature parameter τ in *softmax* to sharpen the distribution:

$$\gamma_{o_s}^{(k)} = \frac{\exp\left(e_{o_s}^{(k)}/\tau\right)}{\sum_{o' \in O_s} \exp\left(e_{o'}/\tau\right)} \tag{12}$$

where o_s is an operation in O_s, and e_{o_s} is its attention score. Through experiments, we set $\tau = 0.1$ to distinguish the preference for the step size in most cases.

A.3 Overhead of A^2

Let the number of steps be K, the number of operations be $|O|$, the image size be $W \times H$ and the embedding size be E. The number of the attacker's parameter is $\mathbf{O}\left(K \cdot E \cdot (W \times H + |O|)\right)$. Specifically, the number of parameters for the attacker is 7873280, which is 17% of the model's parameters (i.e., 46160474). In each batch, there is only 1 forward calculation of all cells with 1 backpropagation. In comparison, the model requires K forward calculations with backpropagation. Therefore, the additional computational overhead from the attacker is not significant in terms of the number of parameters and computations.

Moreover, PGD and A^2 are close in terms of clock time. For WRN-34, PGD takes 19.75/147.09/287.76 seconds to generate 1/10/20 step attacks respectively. It demonstrates that more inner steps lead to a linear increase in time. Meanwhile, A^2 takes 157.61/302.51 seconds to generate the 10/20 step attack respectively. The main overhead remains in the forward computation and backward propagation of the defense model. For WRN-34, the training time of AWP-A^2 is 970 s/epoch while the training time of AWP is 920 s/epoch.

In summary, the additional overhead of A^2 is not significant.

A.4 Why No Mixture in O_p

Like most NAS methods in AutoML, the discrete selection in the perturbation block is more interpretable and robust (e.g., L1-Norm for feature selection and single path in NAS) than the mixture over possible solutions. Moreover, the mixture will incur more computational overhead and 7 times memory overhead due to 7 operations in O_p. Figure 3 shows an example of the generated attack on CIFAR-10, which can be migratable.

B Addition Experiments

B.1 Why use FGSM-based PGD in RQ1.

There are multiple single-step attack methods in O_p for stacking as PGD, e.g., FGM-based PGD and FGSM-based PGD. The experimental results of the attack effect of PGD based on these attack methods demonstrate that FGSM-based PGD outperforms the stacking of other operations. Thus, we

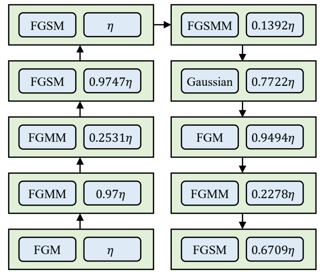

Figure 3: Example of generated attack on CIFAR-10.

choose FGSM-based PGD with a random start $\delta^{(0)} \sim Uniform(-\epsilon, \epsilon)$ as a baseline for comparison with the automated attacker.

B.2 Number of samples M in MC Approximation.

M is an important hyperparameter that dictates the quality of MC approximation and the training overhead. We test the cases with $M \in \{1, 2, 5\}$ and achieve similar performance. Thus, we set M to 1 and achieve good results with a significantly lower overhead.

B.3 Generality of A^2 in White-Box Attacks

Table 5: Comparison of attack effects on CIFAR-10 (%, the lower the better) of PGD-based and CW_∞-based attacks. The architecture of all defense models is WideResNet, except for MART whose architecture is ResNet-18.

	MART	TRADES-AWP	MART-AWP	RST-AWP
Natural	83.07	85.36	85.60	88.25
PGD^{20}	53.76	59.64	59.52	64.14
PGD^{20}-A^2	53.24	59.34	59.25	63.97
CW_∞	49.97	57.07	56.44	61.82
CW_∞-A^2	**49.82**	**56.98**	**55.81**	**61.30**

In this part, we investigate whether A^2 is general to white-box attacks. As a more powerful attack method, CW_∞-based attacks [Carlini and Wagner, 2017] stably outperform PGD-based attacks. For comparison with CW_∞, we propose a variant of A^2 that uses CW_∞ loss to generate perturbations and denote it as CW_∞-A^2. The results in Table 5 show that A^2 is general and can improve the attack effect of PGD and CW_∞ by combining attack methods and tuning the step size. Moreover, the additional overhead of A^2 is 5% to 10%, which is a rather acceptable trade-off.

B.4 Robustness Against Transferable Black-Box Attacks

We investigate the robustness of A^2 against transferable black-box attacks. Table 6 provides test robustness on CIFAR-10 using ResNet-18. We adopt three transferable black-box attack methods: MI (momentum = 1) [Dong et al., 2018], DI [Xie et al., 2019], and TI [Dong et al., 2019]. The transferable attacks are generated by an ensemble of the above methods on three surrogate pre-trained models [2]: IncV3 (InceptionV3), VGG19, and DN201 (DenseNet201). Table 6 shows that AT boosts the robustness against transferable black-box attacks, and A^2 can further improve the adversarial robustness.

Table 6: Test robustness (%, the higher the better) on CIFAR-10 using ResNet-18 against transferable black-box attacks.

	MI+DI+TI			
	IncV3	VGG19	DN201	PGD^{20}
ResNet-18	16.12	7.37	5.35	0.02
ResNet-18-AT	61.98	60.81	59.63	52.79
ResNet-18-AT-A^2	**62.79**	**61.85**	**60.28**	**52.96**

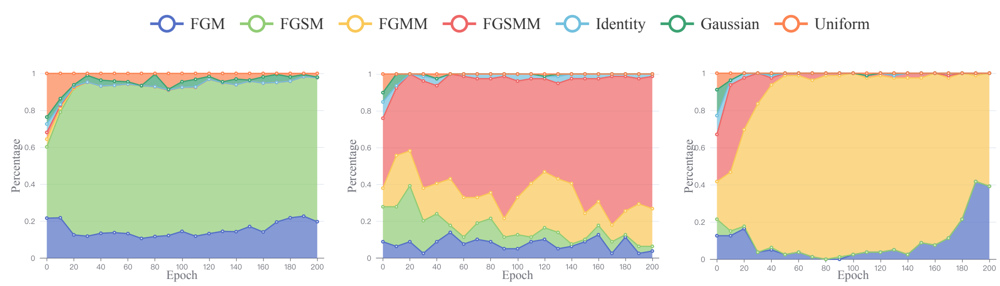

(a) Block 1 in CIFAR-10 (b) Block 10 in CIFAR-10 (c) Block 10 in SVHN

Figure 4: Distribution of attacks selected by perturbation blocks of A^2.

B.5 A Closer Look at Selected Attacks

We analyze the selected attacks from the perspective of perturbation blocks with different steps and datasets.

The first and final perturbation blocks of 10-step A^2 in CIFAR-10 are chosen for analysis. Figure 4 shows the distribution of selected attacks of different perturbation blocks.

- **Perturbation Block 1:** A^2 tends to choose *FGM*, *FGSM*, and partially random methods as initialization in the first step. The momentum-based attack methods are quickly discarded as the gradient of the previous step is absent. *FGSM* is chosen more frequently due to its stronger attack on both foreground and background.
- **Perturbation Block 10:** The optimization of the victim model leads to changes in the distribution of selected attacks in the last block. In the early stage of training, the victim model is vulnerable. A^2 retains the diversity and plays the role of friendly attackers like FAT [Zhang et al., 2020]. At the end of training, A^2 prefers the momentum-based attacks (i.e., *FGSMM* and *FGMM*).

From the perspective of datasets, SVHN and CIFAR-10 prefer different attack methods. As shown in Figure 4(c), SVHN discards *FGSMM*, which is most frequently used in CIFAR-10, and pays more attention to *FGMM*. Moreover, SVHN rarely uses *Identity* compared with CIFAR-10 as its higher robustness accuracy requires more powerful perturbations.

In summary, A^2's preference for selecting attacks in blocks varies according to the block step, dataset, and victim model.

[2] https://github.com/huyvnphan/PyTorch_CIFAR10